Strong particle-hole asymmetry of charge instabilities in doped Mott insulators

2014 New J. Phys. 16 123002

(http://iopscience.iop.org/1367-2630/16/12/123002)

New Journal of Physics
The open access journal at the forefront of physics
Deutsche Physikalische Gesellschaft DPG | IOP Institute of Physics

Strong particle-hole asymmetry of charge instabilities in doped Mott insulators

Matías Bejas[1], Andrés Greco[1] and Hiroyuki Yamase[2,3]
[1] Facultad de Ciencias Exactas, Ingeniería y Agrimensura and Instituto de Física Rosario (UNR-CONICET), Avenida Pellegrini 250, 2000 Rosario, Argentina
[2] National Institute for Materials Science, Tsukuba 305-0047, Japan
[3] Max Planck Institute for Solid State Research, D-70569 Stuttgart, Germany
E-mail: bejas@ifir-conicet.gov.ar, agreco@fceia.unr.edu.ar and yamase.hiroyuki@nims.go.jp

Received 10 July 2014, revised 20 September 2014
Accepted for publication 14 October 2014
Published 2 December 2014
New Journal of Physics **16** (2014) 123002
doi:10.1088/1367-2630/16/12/123002

Abstract
We study possible charge instabilities in doped Mott insulators by employing the two-dimensional t-J model with a positive value of the next nearest-neighbor hopping integral t' on a square lattice, which is applicable to electron-doped cuprates. Although the d-wave charge density wave (flux phase) and d-wave Pomeranchuk instability (nematic order) are dominant instabilities for a negative t' that corresponds to hole-doped cuprates, we find that those instabilities are strongly suppressed and become relevant only rather close to half filling. Instead, various types of bond orders with modulation vectors close to (π, π) are dominant in a moderate doping region. Phase separation is also enhanced, but it can be suppressed substantially by the nearest-neighbor Coulomb repulsion without affecting the aforementioned charge instabilities.

Keywords: electron- and hole-doped cuprates, pseudogap, charge orders

1. Introduction

High-temperature cuprate superconductors are realized by carrier doping into antiferromagnetic Mott insulators, and superconductivity is characterized by d-wave symmetry. The cuprate superconductors are layered materials; and the electronic properties in the CuO_2 plane, where

Cu sites form a square lattice, hold the key to high-temperature superconductivity. Its essential physics is believed to be contained in the two-dimensional t-J and Hubbard models on a square lattice [1, 2]. Despite these common views, the underlying physics of cuprate superconductivity remains highly elusive.

One of the notorious puzzles in hole-doped cuprates (h-cuprates) concerns the pseudogap (PG) [3, 4], a gap-like feature in the normal phase even far above the superconducting onset temperature (T_{sc}). There are two major scenarios for the origin of the PG. One scenario invokes fluctuations of Cooper pairs above T_{sc} [5–7], whereas the other invokes some order competing with superconductivity. Recent angle-resolved photoemission spectroscopy [8–11] observes the two-gap feature in the electronic band dispersion, in favor of the latter scenario for the PG. However, it is a matter of considerable debate what kind of order actually develops in the PG. The so-called YRZ model [12] exploits the concept of the resonating-valence-bond theory [13, 14] and successfully captures some features of the PG. On the other hand, various experimental observations in the PG state are also well captured in terms of charge instabilities such as d-wave charge density wave (dCDW) [15–19], a loop current order [20, 21], d-wave Pomeranchuk instability (dPI) [22–24], conventional charge density wave (CDW) [25–28] including stripes [29, 30], and phase separation (PS) [25, 26, 31].

Quite recently a charge-order instability was observed by X-rays in two different h-cuprates, Y-based [32–34] and Bi-based [35, 36] cuprates. This charge order is not accompanied by a magnetic order, in sharp contrast with the spin-charge stripes [37] discussed extensively in La-based cuprates [29]. Thus, charge-order instabilities in cuprates have attracted renewed interest. A comprehensive study [38] about possible charge orders in the t-J model showed that doped Mott insulators exhibit strong tendencies toward the dCDW and dPI. In particular, the incommensurate dPI [38–45] attracts much interest. However, its modulation vector is not consistent with the experiments [32–36], requiring further study both theoretically and experimentally.

Electrons can also be doped into the parent compound of cuprates. Electron-doped cuprates (e-cuprates) [46], however, look very different from h-cuprates. A PG similar to that found in h-cuprates is not clearly observed. If the PG indeed originates from some charge order, as discussed regarding h-cuprates, it seems natural to assume that charge-order tendencies are strongly suppressed in e-cuprates. On the other hand, a recent finding of collective excitations in optimal e-cuprates [47] suggests that a charge-order tendency can be present.

Electron-doped cuprates have often been discussed via a comparison with h-cuprates, focusing on specific aspects, e.g., pairing properties [48, 49], magnetic properties [50, 51], stability of charge stripes but with different conclusions [48, 52], and optical conductivity [53]. A recent comprehensive study using variational Monte Carlo [54] showed that superconductivity is enhanced but antiferromagnetism is suppressed in h-cuprates, whereas the opposite occurs in e-cuprates, nicely demonstrating the experimental fact. In spite of these works, charge-order tendencies in e-cuprates have not been clarified.

In this paper, we study all possible charge instabilities in e-cuprates in the framework of the two-dimensional t-t'-J model. We employ a similar theoretical framework in which charge-order tendencies have been studied comprehensively for h-cuprates [38]. In this sense, the current work is a complement to [38] and is expected to clarify charge-order tendencies in e-cuprates in the most comprehensive way through a comparison with those in h-cuprates. We find that charge-order tendencies exhibit a very strong particle-hole asymmetry. Although h-cuprates have strong tendencies toward the dCDW and dPI [38], these orders are substantially

suppressed in *e*-cuprates. Instead, various bond orders with large momenta near (π, π) are favored in a moderated doping region. In section 2, we define our model and explain our methods. Numerical results are presented in section 3. We discuss possible charge instabilities and the PG in *e*-cuprates in section 4, followed by conclusions in section 5.

2. Model and formalism

We study charge instabilities in the two-dimensional t-t'-J model by including the nearest-neighbor Coulomb interaction V,

$$H = -\sum_{i,j,\sigma} t_{ij}\tilde{c}^{\dagger}_{i\sigma}\tilde{c}_{j\sigma} + J\sum_{\langle i,j\rangle}\left(\vec{S}_i\cdot\vec{S}_j - \frac{1}{4}n_i n_j\right) + V\sum_{\langle i,j\rangle} n_i n_j. \tag{1}$$

$t_{ij} = t$ (t') is the hopping integral between the first (second) nearest-neighbor sites on a square lattice; J and V are the exchange interaction and the Coulomb repulsion, respectively, between the nearest-neighbor sites. $\langle i, j\rangle$ indicates a nearest-neighbor pair. $\tilde{c}^{\dagger}_{i\sigma}$ and $\tilde{c}_{i\sigma}$ are the creation and annihilation operators of electrons with spin σ $(\sigma = \downarrow, \uparrow)$, respectively, in Fock space without any double occupancy. $n_i = \sum_{\sigma}\tilde{c}^{\dagger}_{i\sigma}\tilde{c}_{i\sigma}$ is the electron density operator and $\vec{S}_i$ is the spin operator in that space. Although the V term is usually neglected in the analysis of the t-J model, its presence is natural, as seen in the derivation of the t-J model from the generalized Hubbard model [55]. We found that a role of the V term in the current study is to suppress the strong tendency toward PS (see section 3.2) and does not affect the charge instabilities originating from the J term (see section 3.3). There are higher-order corrections to the t-J model, such as correlated hopping terms [55, 56]. We expect that those corrections do not blur our principal physics originating from the J term as well as the strong correlation effect contained in (1). We thus discard them in the current study.

We study the Hamiltonian (1) in a large-N technique formulated in a path integral representation of the Hubbard X operators [38, 57]. Because details of the formalism were presented in [38], we provide a simple sketch of that here.

We first write the Hamiltonian (1) in terms of Hubbard operators [58] via $\tilde{c}^{\dagger}_{i\sigma} = X_i^{\sigma 0}$, $\tilde{c}_{i\sigma} = X_i^{0\sigma}$, $S_i^{+} = X_i^{\uparrow\downarrow}$, $S_i^{-} = X_i^{\downarrow\uparrow}$, $S_i^{z} = (X_i^{\uparrow\uparrow} - X_i^{\downarrow\downarrow})/2$, and $n_i = X_i^{\uparrow\uparrow} + X_i^{\downarrow\downarrow}$; X_i^{00} will also be introduced later (see (4)). We then extend the spin degree of freedom to N channels and obtain the Hamiltonian in the large-N formalism,

$$H_N = -\frac{1}{N}\sum_{i,j,p} t_{ij}X_i^{p0}X_j^{0p} + \frac{J}{2N}\sum_{\langle i,j\rangle,pp'}\left(X_i^{pp'}X_j^{p'p} - X_i^{pp}X_j^{p'p'}\right) + \frac{V}{N}\sum_{\langle i,j\rangle,pp'} X_i^{pp}X_j^{p'p'} - \mu\sum_{i,p} X_i^{pp}. \tag{2}$$

The spin index σ is extended to a new index p, which runs from 1 to N. To obtain a finite theory in the N-infinite limit, t, t', J, and V are rescaled as t/N, t'/N, J/N, and V/N, respectively. The chemical potential μ is introduced in (2).

The Hamiltonian (2) can be formulated in a path integral representation [57]. Our Euclidean Lagrangian then reads

$$L_E = \frac{1}{2}\sum_{i,p}\frac{\left(\dot{X}_i^{0p}\, X_i^{p0} + \dot{X}_i^{p0}\, X_i^{0p}\right)}{X_i^{00}} + H_N \tag{3}$$

with the following two additional constraints,

$$X_i^{00} + \sum_p X_i^{pp} - \frac{N}{2} = 0 \tag{4}$$

and

$$X_i^{pp'} - \frac{X_i^{p0} X_i^{0p'}}{X_i^{00}} = 0, \tag{5}$$

which are imposed on the path integral via two δ-functions. In (3), $\dot{X}_i^{p0} = \partial_\tau X_i^{p0}$ and τ is the Euclidean time, namely $\tau = \mathrm{i}t$.

We first write X_i^{pp} in the Hamiltonian (2) in terms of X_i^{00} by using (4). This ensures that the V term vanishes at half filling due to strong correlation effects in the Mott insulator. The completeness condition (4) imposed by the δ function is now described by introducing Lagrange multipliers λ_i. We describe X_i^{00} and λ_i in terms of static mean-field values, r_0 and λ_0, and fluctuation fields, δR_i and $\delta\lambda_i$:

$$\begin{aligned} X_i^{00} &= N r_0\left(1 + \delta R_i\right) \\ \lambda_i &= \lambda_0 + \delta\lambda_i. \end{aligned} \tag{6}$$

From the completeness condition (4), r_0 is equal to $\delta/2$, where δ is the doping rate away from half filling. We then eliminate $X^{pp'}$ by implementing the δ-function associated with (5). This procedure creates interaction terms such as $X_i^{p0} X_i^{0p'} X_j^{p'0} X_j^{0p}$, which are decoupled through a Hubbard-Stratonovich transformation by introducing a field associated with a bond variable,

$$\Delta_{ij} = \frac{J}{N r_0}\sum_p \frac{X_j^{p0} X_i^{0p}}{\sqrt{\left(1 + \delta R_i\right)\left(1 + \delta R_j\right)}}. \tag{7}$$

The field Δ_{ij} is parameterized by

$$\Delta_i^\eta = \Delta\left(1 + r_i^\eta + \mathrm{i}A_i^\eta\right), \tag{8}$$

where r_i^η and A_i^η correspond to the real and imaginary parts of the fluctuations of the bond variable, respectively, and Δ is a static mean-field value. The index η takes two values associated with the bond directions $\eta_1 = (1, 0)$ and $\eta_2 = (0, 1)$ on a square lattice. After expanding $1/(1 + \delta R)$ in powers of δR, we obtain an effective Lagrangian, which can be written in terms of a six-component bosonic field

$$\delta X^a = (\delta R,\ \delta\lambda,\ r^{\eta_1},\ r^{\eta_2},\ A^{\eta_1},\ A^{\eta_2}), \tag{9}$$

the fermionic fields X^{0p} and X^{p0}, and their interactions. Any physical quantity can then be calculated at a given order by counting powers of $1/N$ in a corresponding Feynman diagram, providing a controllable scheme. The Feynman rules are given in figure 1 in [57].

Because the bosonic field has six components (see (9)), its bare propagator $D_{ab}^{(0)}(\mathbf{q}, \mathrm{i}\omega_n)$ is given by a 6×6 matrix; $\mathbf{q}$ and $\mathrm{i}\omega_n$ are the momentum and bosonic Matsubara frequency, respectively. The quantity $D_{ab}^{(0)}(\mathbf{q}, \mathrm{i}\omega_n)$ describes all possible types of bare charge

susceptibilities. From the Dyson equation, the dressed propagator is given by

$$D_{ab}^{-1}(\mathbf{q}, \mathrm{i}\omega_n) = \left[D_{ab}^{(0)}(\mathbf{q}, \mathrm{i}\omega_n)\right]^{-1} - \Pi_{ab}(\mathbf{q}, \mathrm{i}\omega_n). \tag{10}$$

The bosonic propagator acquires the self-energy $\Pi_{ab}(\mathbf{q}, \mathrm{i}\omega_n)$ already at the leading order (see equations (15)–(18) in [38] for the explicit expression of $D_{ab}^{-1}(\mathbf{q}, \mathrm{i}\omega_n)$). As a result, an eigenvalue of $D_{ab}(\mathbf{q}, 0)$ can diverge, leading to a charge instability with a modulation vector $\mathbf{q}$.

From the N-extended completeness condition (4), we see that the charge operator X^{00} is $O(N)$, whereas the operators X^{pp} are $O(1)$. Consequently, the $1/N$ approach emphasizes the effective charge interactions. In fact, collective effects enter the spin susceptibilities in the next-to-leading order. This is also the case for superconductivity [16]. Hence instabilities of the paramagnetic phase are expected only, in the leading order, in the charge sector. This is an advantage of our method and allows us to explore all possible charge instabilities exclusively. We therefore retain our approximation at the leading order. In the leading order theory, however, we cannot address the ground state, which likely exhibits superconductivity. Hence our results should be interpreted as microscopic indications of what kind of charge instabilities become relevant in a parameter region where magnetism and superconductivity are absent.

In the leading order, our formalism agrees with the $1/N$ slave-boson formalism [59] as well as results in another formalism of the $1/N$ expansion [16]. Our formalism was also verified, in the next-to-leading order, to yield results consistent with exact diagonalization [60, 61]. In the next section, we will also pay attention to the consistency between our results and existing literature.

3. Results

The t-t'-J model with $t' < 0$ has been extensively studied in the context of h-cuprates. Because the model is defined in Fock space without any double occupancy, we perform a particle-hole transformation [50] for studying e-cuprates. This is implemented by taking a positive value of t' [48–53].

In the following, we set $t = 1$, and all quantities with the dimension of energy are in units of t except for figure 6. A typical value of t in cuprates is estimated to be around 500 meV [62].

3.1. Possible charge instabilities in e-cuprates

We compute the static charge susceptibilities $D_{ab}(\mathbf{q}, 0)$ from (10), which are given by a 6×6 matrix, at the leading order of the large-N expansion. When an eigenvalue of the inverse of the matrix, namely $D_{ab}^{-1}(\mathbf{q}, 0)$, crosses zero at a given doping rate δ, temperature T, and $\mathbf{q}$, a charge instability with a modulation vector $\mathbf{q}$ occurs and the ordering pattern is determined by the corresponding eigenvector V^a. The eigenvectors that we have found are the same as those in [38], although we employ the opposite sign of t' here. We explain these eigenvectors one by one in the following paragraphs.

(i) $V^a \propto (0, 0, 0, 0, 1, -1)$, which corresponds to the dCDW (flux phase) with $\mathbf{q} = (\pi, \pi)$ [16, 57, 59, 63, 64]. In this phase, currents flow in each plaquette as shown in figure 1(a).

(ii) $V^a \propto (0, 0, 1, -1, 0, 0)$, which corresponds to a dPI with $\mathbf{q} = (0, 0)$ (commensurate) [65–67] or close to it (incommensurate) [38–45]. The dPI leads to the electronic nematic state as an instability of the paramagnetic state. The commensurate and the incommensurate dPI are shown in figures 1(b) and (c), respectively.

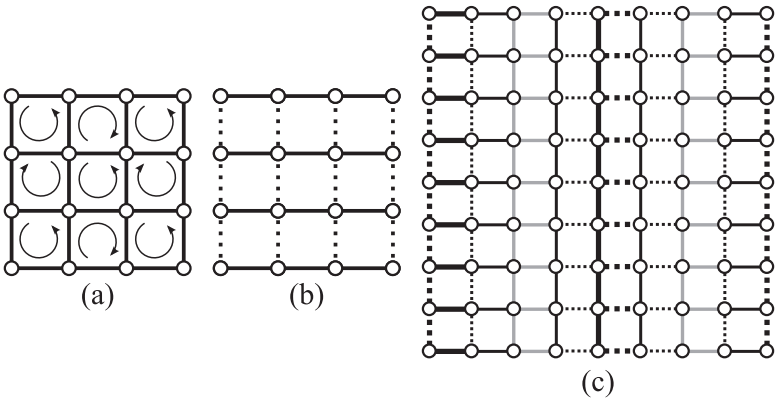

Figure 1. Sketch of (a) *d*CDW with $\mathbf{q} = (\pi, \pi)$, (b) *d*PI with $\mathbf{q} = (0, 0)$, and (c) *d*PI with $\mathbf{q} = (\pi/4, 0)$. The black lines in (b) and (c) denote a stronger (solid line) and weaker (dotted line) bond relative to the mean-field bond variable (gray line), namely the constant term on the right-hand side of (8). The width of the lines in (c) indicates the modulation amplitude.

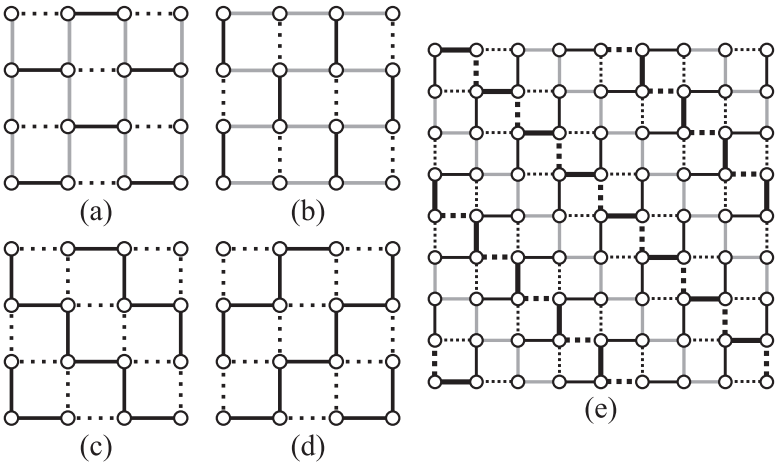

Figure 2. Sketch of (a) BOP_x, (b) BOP_y, (c) BOP_{xy}, and (d) $\mathrm{BOP}_{x\bar{y}}$ for $\mathbf{q} = (\pi, \pi)$; (e) $\mathrm{BOP}_{x\bar{y}}$ with $\mathbf{q} = (3\pi/4, 3\pi/4)$. Gray, solid, and dotted lines are explained in figure 1.

(iii) $V^a \propto (0, 0, 1, 0, 0, 0)$, $(0, 0, 0, 1, 0, 0)$, $(0, 0, 1, 1, 0, 0)$, and $(0, 0, 1, -1, 0, 0)$, which correspond to the bond-order phase (BOP) [16, 57, 59] with $\mathbf{q} = (\pi, \pi)$ or close to it, with four different patterns: BOP_x, BOP_y, BOP_{xy}, and $\mathrm{BOP}_{x\bar{y}}$, respectively (see figures 2(a)–(d)). $\mathrm{BOP}_{x(y)}$ is a phase that has a bond amplitude modulated only along the $x(y)$ direction, whereas $\mathrm{BOP}_{xy(x\bar{y})}$ with (π, π) has a bond amplitude modulated along both the x and y directions, and its relative phase is inphase (antiphase). Because the *d*PI and $\mathrm{BOP}_{x\bar{y}}$ belong to the same eigenvector $(0, 0, 1, -1, 0, 0)$, the *d*PI with $\mathbf{q} \approx (\pi, \pi)$ is equivalent to the $\mathrm{BOP}_{x\bar{y}}$. However, the term of the *d*PI makes sense only for a small $\mathbf{q}$, and thus we use the term $\mathrm{BOP}_{x\bar{y}}$ when $\mathbf{q}$ is no longer close to $(0, 0)$. We also sketch $\mathrm{BOP}_{x\bar{y}}$ with $\mathbf{q} = (3\pi/4, 3\pi/4)$ in figure 2(e). Such an order can occur for a large t' (see figure 5).

(iv) $V^a \propto (1, 0, 0, 0, 0, 0)$, which corresponds to a PS with $\mathbf{q} = (0, 0)$. Conventional CDW including charge stripes also belongs to the same eigenvector, but with a finite $\mathbf{q}$. Such an

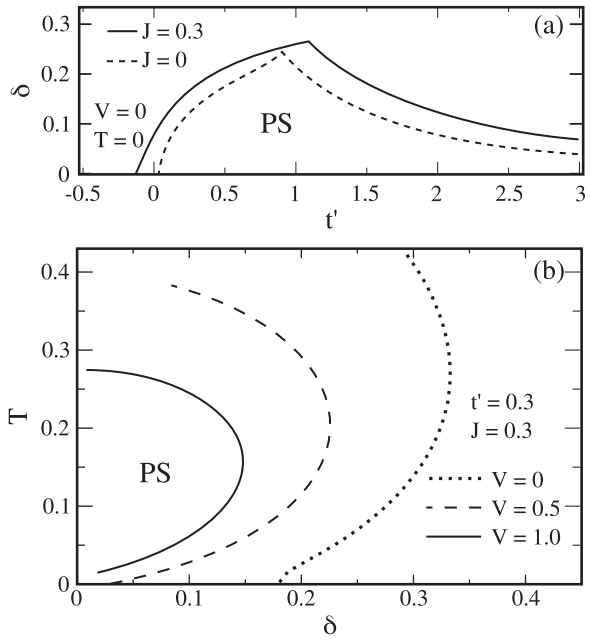

Figure 3. (a) Phase separation in the plane of t' and δ for $J = 0$ and 0.3 at $V = T = 0$. (b) Phase separation in the plane of δ and T for various V at $J = 0.3$ and $t' = 0.3$.

instability was not found in the current study. This work is in favor of [48] more than [52] regarding the stability of charge stripes.

In the following, we will specify a parameter region where each charge instability can occur by varying doping rate δ, temperature T, and the next-nearest neighbor hopping t'. Because we determine critical lines of charge instabilities by studying susceptibility, the transition is always continuous and a possible first-order transition is not considered in the current study.

Before presenting our results, we emphasize that our general susceptibility (10) considers all possible charge instabilities. As mentioned in the Introduction, various charge instabilities are discussed in the context of the PG, and most of them are indeed found in this work except for conventional CDW including stripes; the loop current order is beyond the scope of the one-band *t-J* model. A bond-order modulated flux phase was discussed in variational Monte Carlo in the *t-J* model at zero temperature [68, 69]. Such a state is described by the mixture of two eigenvectors, (0, 0, 0, 0, 1, −1) and (0, 0, 1, 1, 0, 0), in the current theory but is not found here. This suggests that such a state may not occur as an instability from the normal phase but may occur as an additional instability inside the symmetry broken phase characterized by either eigenvector. This possibility cannot be addressed in the current theory because we perform the stability analysis of the normal phase in terms of susceptibility.

3.2. Phase separation

We first discuss PS. As seen in the literature [49, 51, 70], PS is strongly enhanced for a positive t'. Figure 3(a) shows PS in the plane of t' and δ at $V = T = 0$ for $J = 0$ and 0.3; $\delta = 0$ corresponds to half filling, and δ denotes the electron (hole) doping rate for $t' > 0 (< 0)$. As seen from the large slope at $t' \approx -0.1$ for $J = 0.3$, PS is rapidly stabilized with increasing

t' (> -0.1) and extends to 15% doping already around $t' \approx 0.1$. PS is monotonically enhanced up to $t' \approx 1$ and is suppressed for $t' > 1$. A similar result was also obtained by exact diagonalization [49]. Although PS is enhanced by the J term, the t' dependence of PS is well captured by the result of $J = 0$. Although one might assume that a finite J is necessary to obtain PS, the kinetic term in the t-J model (first term in the Hamiltonian (1) and (2)) is not a usual non-interacting term but already contains strong correlation effects coming from the local constraints (4) and (5). Figure 3 thus clearly demonstrates that PS originates from strong correlation effects, in line with the result obtained by the dynamical cluster approximation in the strong coupling Hubbard model [70].

Figure 3(b) shows the region of PS in the plane of δ and T for several choices of V at $J = 0.3$ and $t' = 0.3$. PS occurs on the left side of the critical line. As expected, PS is substantially suppressed by increasing V. We verified that no additional CDW instability was triggered for the current values of V. The doping region of PS shrinks at low and high T. Because of such reentrant behavior, PS can be stabilized at a finite T even if it does not occur at $T = 0$. A result similar to figure 3(b) was also obtained in the Hubbard model in strong coupling [71]. We, however, note that our PS is not a pure PS especially for high T. Although the eigenvector of PS contains the component of (1, 0, 0, 0, 0, 0) almost 100% close to zero temperature, the weight from other components, especially from (0, 0, 1, 1, 0, 0), increases with increasing T. For example, the weight of the (1, 0, 0, 0, 0, 0) component is reduced to about 80% (50%) at $T = 0.1\,(0.2)$ for $V = 1.0$; such a reduction occurs at a higher temperature for a smaller V.

Given that PS tendencies found here are consistent with results obtained in other methods [49, 51, 70, 71] we believe that PS is a genuine feature of the t-J model. However, when PS occurs, charge accumulates in one region more than in the other region. In this case, it is readily expected that long-range Coulomb interaction, which is not considered in the t-J model, may stabilize an inhomogeneous state. This possibility is worth exploring further.

3.3. Charge instabilities from the J term

We now study all the other possible charge instabilities and fix $J = 0.3$, which is believed to be appropriate to cuprates [50, 51, 62]. We choose $V = 1$ to suppress PS, but charge instabilities from the J term turn out to be rather insensitive to the choice of V. The latter aspect of the V term might be surprising from the point of view of weak coupling theory. However, as seen in our formalism in section 2, the V term vanishes at half filling and the current theory belongs to a strong coupling theory formulated in terms of the Hubbard X operators. The value of t' is estimated to be around $t' = 0.2 \sim 0.4$ for e-cuprates [50, 51, 62]. Because a realistic value of t is around 500 meV in cuprates [62], the temperature range we are interested in is below $T = 0.04$–0.02, which corresponds to a region below 200–100 K.

Figure 4 shows a phase diagram in the plane of δ and T. It extends the information we obtained in figure 2 of [38] for h-cuprates by showing the effect of a positive t' appropriate for e-cuprates. As already seen in figure 3(b), PS occurs on the side of half filling and is enhanced at high T. In contrast with PS, other charge instabilities are driven by the J term. In figure 4(a), they occur at lower temperatures ($0 < T < 0.04$) below $\delta \approx 0.14$. This region is actually what we are interested in, in the context of e-cuprates. We obtain three different types of charge instabilities: dCDW with $\mathbf{q} = (\pi, \pi)$, dPI with $\mathbf{q} = (0, 0)$, and various BOPs such as $\mathrm{BOP}_{x\,(y)}$, BOP_{xy}, and $\mathrm{BOP}_{x\bar{y}}$ with $\mathbf{q} \approx (\pi, \pi)$. The dPI is suppressed most strongly and is stabilized only

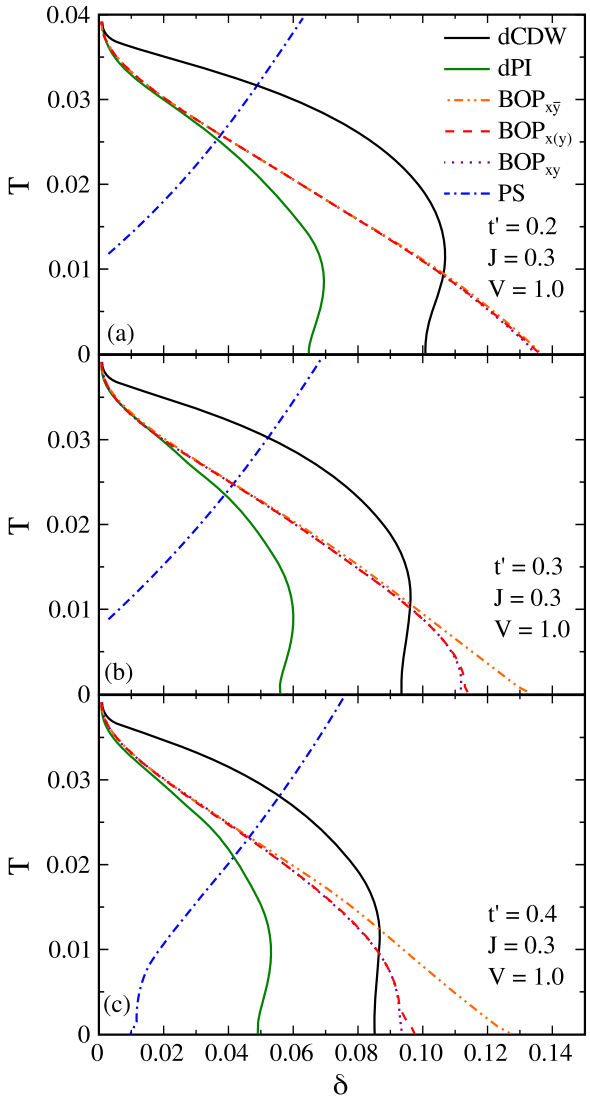

Figure 4. Doping dependence on critical temperatures T_c of dCDW, dPI, BOP$_{x\bar{y}}$, BOP$_{x(y)}$, BOP$_{xy}$, and PS for $J = 0.3$ and $V = 1$; (a) $t' = 0.2$, (b) 0.3, and (c) 0.4. The instability occurs below the corresponding critical line except for PS, which is stabilized on the left side of the critical line.

rather close to half filling. Although the dCDW is the leading instability in $\delta \lesssim 0.1$, BOP$_{x(y)}$, BOP$_{xy}$, and BOP$_{x\bar{y}}$ become dominant in the region $0.1 \leqslant \delta \leqslant 0.14$ and show instabilities almost simultaneously. As t' increases, charge instabilities except for PS are suppressed and stabilized closer to half filling, as seen in figures 4(b) and (c). Among various BOPs, BOP$_{x\bar{y}}$ becomes the leading instability at low T in a moderate doping region with increasing t'. We verified that the results of figure 4, except for PS, do not depend on a precise choice of the value of V. Because we compute the general susceptibility in the paramagnetic state, figure 4 should be interpreted as a hierarchy of different charge instabilities. For instance, in figure 4(c) at $\delta = 0.08$, dCDW and BOP$_{x\bar{y}}$ are the leading and next-to-leading instabilities, respectively. BOP$_{x(y)}$ and BOP$_{xy}$ are degenerate and the third-to-leading instability.

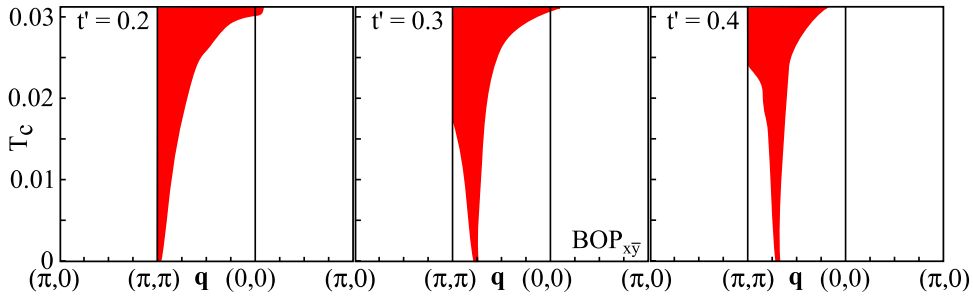

Figure 5. Modulation vectors of BOP$_{x\bar{y}}$ along the corresponding critical lines in figure 4.

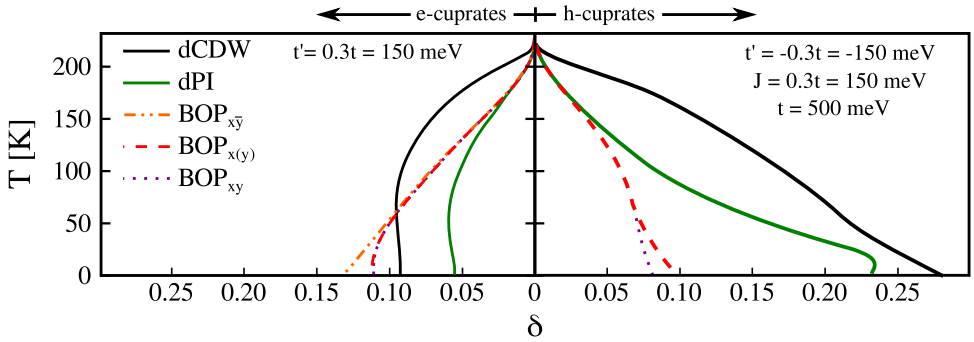

Figure 6. Comparison between the current results for *e*-cuprates (left panel), which is the same as figure 4(b), and the previous results [38] for *h*-cuprates (right panel). Using $t = 500$ meV, the temperature scale is given in K for easy comparison with experiments.

Although the *d*PI and *d*CDW instabilities always occur at $\mathbf{q} = (0, 0)$ and (π, π), respectively, the modulation vectors of BOP$_{xy}$ and BOP$_{x(y)}$ show the instabilities at $\mathbf{q} = (\pi, \pi)$ and shift at very low T ($\lesssim 0.005$) slightly toward the direction (π, π)–$(\pi, 0)$ for BOP$_{xy}$ and BOP$_x$ and the direction (π, π)–$(0, \pi)$ for BOP$_y$. The modulation vector of BOP$_{x\bar{y}}$ is shown in figure 5 along its critical line in figures 4(a)–(c); hence the doping rate also changes with changing T_c. In contrast with the case of BOP$_{xy}$ and BOP$_{x(y)}$, the charge susceptibility corresponding to BOP$_{x\bar{y}}$ is rather flat in momentum space. We thus plot the modulation vectors where the inverse of the charge susceptibility is less than 10^{-4}. The width of such a $\mathbf{q}$ region at a fixed temperature indicates how sharp the susceptibility is in momentum space. The modulation vector does not extend to the side of the (π, π)–$(\pi, 0)$ direction because the eigenvector there changes to BOP$_x$. As T decreases, the susceptibility becomes sharper. The modulation vector then becomes $\mathbf{q} = (\pi, \pi)$ for $t' = 0.2$ and shifts toward the diagonal direction along (π, π)–$(0, 0)$ for a larger t'.

Compared with the results for $t' < 0$ obtained in [38], charge instabilities, except for PS, show a much weaker dependence on t' for $t' > 0$. To show explicitly the strong particle-hole asymmetry of charge instabilities, we compare in figure 6 the current results for $t' = 0.3$ with our previous results for *h*-cuprates obtained in [38] for the same parameter set except for the sign of t'. Although the tendencies of BOPs are even weaker than those of the *d*PI and *d*CDW for $t' < 0$, various BOPs extend to a moderate doping for $t' > 0$ and become dominant there. Both the *d*CDW and the *d*PI are strongly suppressed for *e*-cuprates compared with *h*-cuprates.

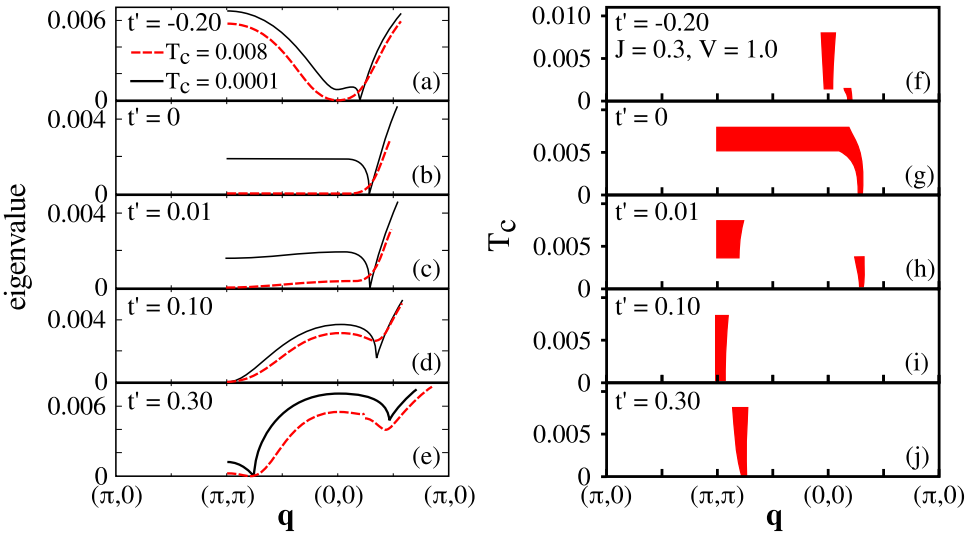

Figure 7. (a)–(e) **q** dependence on the eigenvalue corresponding to the eigenvector (0, 0, 1, −1, 0, 0) at the critical temperatures $T_c = 0.008$ and 0.0001 for a sequence of t'. The instability occurs when the eigenvalue crosses zero. (f)–(j) T_c dependence of the modulation vector **q** of the charge instability with the eigenvector (0, 0, 1, −1, 0, 0). The result (j) is the same as figure 5 for $t' = 0.3$ in a low-temperature region.

Whereas the *d*CDW can be still a relevant instability in *e*-cuprates, the tendency toward the *d*PI becomes the weakest when the sign of t' is reversed. To understand such a drastic change for the *d*PI, we closely study how the modulation vector of the *d*PI evolves by changing t'. In the left-hand panels in figure 7, we show the eigenvalue of the inverse of the susceptibility for the eigenvector (0, 0, 1, −1, 0, 0) at $T_c = 0.008$ and 0.0001 for a sequence of t'. In the right-hand panels, the corresponding modulation vector **q** is summarized by determining the momentum **q** at which the eigenvalue becomes less than 10^{-4} at each temperature. For $t' = -0.2$ (figures 7(a) and (f)) the *d*PI occurs at $\mathbf{q} = (0, 0)$ and slightly away from it at very low T. For $t' = 0$ (figures 7(b) and (g)) the susceptibility of the *d*PI becomes flat along the direction (0, 0)–(π, π), but eventually an incommensurate **q** is favored along the direction (0, 0)–$(\pi, 0)$ at low T. The flat feature is a special aspect of the *d*PI susceptibility, which becomes exactly flat along the (0, 0)–(π, π) direction for any T and δ for $t' = 0$ [38]. With the inclusion of a tiny $t'(= 0.01)$ (figure 7(c)), the flat structure is slightly slanted and the eigenvalue at $\mathbf{q} = (\pi, \pi)$ becomes smaller than that at (0, 0). As a result, the instability occurs at $\mathbf{q} = (\pi, \pi)$ at high T, which is equivalent to $\mathrm{BOP}_{x\bar{y}}$. Although the flat feature still remains at low T (figure 7(c)), an incommensurate *d*PI develops along the direction of (0, 0)–$(\pi, 0)$, similar to the results for $t' = 0$. A value of $t' \geqslant 0.10$ is sufficient to completely destroy the *d*PI with a small **q** and stabilizes $\mathrm{BOP}_{x\bar{y}}$ with $\mathbf{q} \approx (\pi, \pi)$ in the entire temperature region (figures 7(i) and (j)). The eigenvalue[1], however, still has a local minimum along (0, 0)–$(\pi, 0)$ (figures 7(d) and (e)). These results, therefore, imply that the reason why the stabilization of the *d*PI changes rapidly by changing the sign of t' lies in the special feature of the *d*PI susceptibility, which exhibits an exactly flat structure along the (0, 0)–(π, π) direction for $t' = 0$.

[1] When **q** changes from (0, 0) to the direction of $(\pi, 0)$ in figures 7(d) and (e), other components start to mix maximally 5% with the eigenvector (0, 0, 1, −1, 0, 0).

4. Discussions

The *e*-cuprates are characterized by a positive t' in the t-t'-J model [48–53]. We first consider possible effects of superconductivity and antiferromagnetism on our phase diagram, which are not taken into account in our leading order theory. Typically, superconductivity in *e*-cuprates occurs below 25 K [46], which is around 0.004 t in the current theory for $t \sim 500$ meV [62]. Because our charge-order instabilities occur higher than this temperature, a major part of our results could not be affected by superconductivity, although charge orders or their tendencies would be suppressed inside the superconducting state. On the other hand, antiferromagnetism extends to the region of 11–14% doping in e-cuprates [46]. Because charge orders occur below 13–14% in our phase diagram, most of the charge orders that we have found could be masked by antiferromagnetism; yet they can be observed in $Pr_{1-x}LaCe_xCuO_4$, which has a lower critical doping rate of antiferromagnetism. The most relevant charge orders in a moderate doping region are various BOPs with $\mathbf{q}$ close to (π, π), which become dominant below $T \sim 0.01t \sim 50$ K, as seen in figure 4. Figure 4 also implies that the dCDW can become relevant to *e*-cuprates if the critical temperature of antiferromagnetism becomes lower than T_c of the dCDW in a certain doping region. At present, experimental evidence of neither BOP nor dCDW is obtained in *e*-cuprates. However, given that evidence of some order competing with superconductivity was obtained quite recently in *e*-cuprates [72] and that a new type of charge order was also found quite recently in *h*-cuprates [32–36], it may be too early to reach a conclusion about a possible charge instability in *e*-cuprates. In particular, BOPs with $\mathbf{q}$ close to (π, π) are not reported in *h*-cuprates, and thus in this sense *e*-cuprates are attractive for exploring a new type of charge order in cuprates. Even if charge-order instability does not occur, its fluctuation effect can be observed as collective excitations. It is interesting to explore a possible connection with the new collective mode recently found in optimal *e*-cuprates by resonant inelastic X-ray scattering [47].

There is growing evidence that the PG is related to some charge order or its fluctuations in *h*-cuprates [8–11, 73, 74]. In particular, the dCDW [15, 17–19] and dPI [22–24] are candidates. If the charge order is indeed responsible for the PG, the current theory suggests that the property of the PG should be different between hole doping and electron doping because of the strong particle-hole asymmetry of charge-order instabilities. Although a PG was reported in the optical conductivity spectra in the non-superconducting crystals of *e*-cuprates [75], the PG corresponding to the PG observed in *h*-cuprates, namely in a doping region where the superconducting phase occurs at low T, seems to be missing or at least much weaker. It is quite interesting to study whether other scenarios of the PG such as fluctuations associated with Cooper pairing and antiferromagnetism can provide a natural explanation of the asymmetry of the PG between hole-doped and electron-doped cuprate superconductors.

5. Conclusions

We have performed a stability analysis of the paramagnetic phase in the two-dimensional t-t'-J model by employing a leading order theory formulated in a large-N expansion scheme. Our theoretical framework has the advantage of taking into account all possible charge instabilities on equal footing and of allowing us to perform a comprehensive study of charge instabilities in a controllable scheme. We have taken a positive value of t' and our results can be relevant to *e*-

cuprates. To the best of our knowledge, no systematic studies of charge instabilities have been performed for *e*-cuprates, even in the large-N expansion. We have found that the *d*CDW and *d*PI become relevant rather close to half filling and that various types of BOPs with $\mathbf{q}$ close to (π, π) are dominant in a moderate doping region. PS is also enhanced but can be suppressed substantially by the nearest-neighbor Coulomb repulsion V, although the instabilities associated with BOPs, the *d*CDW, and the *d*PI are almost intact even in the presence of large V.

The charge order tendencies we have found for $t' > 0$ are very different from those for $t' < 0$ [38]. This strong particle-hole asymmetry implies that charge orders are less favorable in *e*-cuprates, although they can still occur. Furthermore, if charge orders are responsible for the PG, the current theory may naturally explain the reason why the PG phenomenon is very different between *e*-cuprates and *h*-cuprates.

Acknowledgments

The authors thank A M Oles for a critical reading of the manuscript. AG thanks the National Institute for Materials Science (NIMS), where this work was initiated, and the Max Planck Institute for hospitality. HY was supported by a Grant-in-Aid for Scientific Research from Monkasho and the Alexander von Humboldt Foundation.

References

[1] Anderson P W 1987 *Science* **235** 1196
[2] Zhang F C and Rice T M 1988 *Phys. Rev.* B **37** 3759
[3] Timusk T and Statt B 1999 *Rep. Prog. Phys.* **62** 61
[4] Norman M R, Pines D and Kallin C 2005 *Adv. Phys.* **54** 715
[5] Emery V J and Kivelson S A 1995 *Nature* **374** 434
[6] Norman M R, Kanigel A, Randeria M, Chatterjee U and Campuzano J C 2007 *Phys. Rev.* B **76** 174501
[7] Mishara V, Chatterjee U, Campuzano J C and Norman M R 2014 *Nat. Phys.* **10** 357
[8] Tanaka K *et al* 2006 *Science* **314** 1910
[9] Vishik I M, Lee W S, He R H, Hashimoto M, Hussain Z, Devereaux T P and Shen Z X 2010 *New J. Phys.* **12** 105008
[10] Kondo T, Hamaya Y, Palczewski A D, Takeuchi T, Wen J S, Xu Z J, Gu G, Schmalian J and Kaminski A 2011 *Nat. Phys.* **7** 21
[11] Yoshida T, Hashimoto M, Vishik I M, Shen Z X and Fujimori A 2012 *J. Phys. Soc. Jpn.* **81** 011006
[12] Yang K Y, Rice T M and Zhang F C 2006 *Phys. Rev.* B **73** 174501
[13] Anderson P W, Lee P A, Randeria M, Rice T M, Trivedi N and Zhang F C 2004 *J. Phys.: Condens. Matter* **16** R755
[14] Lee P A, Nagaosa N and Wen X G 2006 *Rev. Mod. Phys.* **78** 17
[15] Chakravarty S, Laughlin R B, Morr D K and Nayak C 2001 *Phys. Rev.* B **63** 094503
[16] Cappelluti E and Zeyher R 1999 *Phys. Rev.* B **59** 6475
[17] Greco A 2009 *Phys. Rev. Lett.* **103** 217001
[18] Bejas M, Buzon G, Greco A and Foussats A 2011 *Phys. Rev.* B **83** 014514
[19] Greco A and Bejas M 2011 *Phys. Rev.* B **83** 212503
[20] Varma C M 1999 *Phys. Rev. Lett.* **83** 3538
[21] Varma C M 2006 *Phys. Rev.* B **73** 155113
[22] Yamase H 2009 *Phys. Rev.* B **79** 052501
[23] Hackl A and Vojta M 2009 *Phys. Rev.* B **80** 220514(R)

[24] Yamase H and Metzner W 2012 *Phys. Rev. Lett.* **108** 186405
[25] Castellani C, Castro C D and Grilli M 1995 *Phys. Rev. Lett.* **75** 4650
[26] Becca F, Tarquini M, Grilli M and Castro C D 1996 *Phys. Rev.* B **54** 12443
[27] Hashimoto M *et al* 2010 *Nat. Phys.* **6** 414
[28] He R H *et al* 2011 *Science* **331** 1579–83
[29] Kivelson S A, Bindloss I P, Fradkin E, Oganesyan V, Tranquada J M, Kapitulnik A and Howald C 2003 *Rev. Mod. Phys.* **75** 1201
[30] Vojta M 2009 *Adv. Phys.* **58** 699
[31] Emery V J and Kivelson S A 1993 *Physica* C **209** 597
[32] Wu T, Mayaffre H, Krämer S, Horvatić M, Berthier C, Hardy W N, Liang R, Bon D A and Julien M H 2011 *Nature* **477** 191
[33] Ghiringhelli G *et al* 2012 *Science* **337** 821
[34] Chang J *et al* 2012 *Nat. Phys.* **8** 871
[35] Comin R, Frano A *et al* 2014 *Science* **343** 390
[36] da Silva Neto E H *et al* 2014 *Science* **343** 393
[37] Tranquada J M, Sternlieb B J, Axe J D, Nakamura Y and Uchida S 1995 *Nature (London)* **375** 561
[38] Bejas M, Greco A and Yamase H 2012 *Phys. Rev.* B **86** 224509
[39] Metlitski M A and Sachdev S 2010 *Phys. Rev.* B **82** 075127
[40] Metlitski M A and Sachdev S 2010 *New J. Phys.* **12** 105007
[41] Holder T and Metzner W 2012 *Phys. Rev.* B **85** 165130
[42] Husemann C and Metzner W 2012 *Phys. Rev.* B **86** 085113
[43] Efetov K B, Meier H and Pépin C 2013 *Nat. Phys.* **9** 442
[44] Bulut S, Atkinson W A and Kampf A P 2013 *Phys. Rev.* B **88** 155132
[45] Sachdev S and Placa R L 2013 *Phys. Rev. Lett.* **111** 027202
[46] Armitage N P, Fournier P and Greene R L 2010 *Rev. Mod. Phys.* **82** 2421
[47] Lee W S *et al* 2014 *Nat. Phys.* **10** 883
[48] White S R and Scalapino D J 1999 *Phys. Rev.* B **60** R753
[49] Martins G B, Xavier J C, Arrachea L and Dagotto E 2001 *Phys. Rev.* B **64** R180513
[50] Tohyama T and Maekawa S 1994 *Phys. Rev.* B **49** 3596
[51] Gooding R J, Vos K J E and Leung P W 1994 *Phys. Rev.* B **50** 866
[52] Tohyama T, Gazza C, Shih C T, Chen Y C, Lee T K, Maekawa S and Dagotto E 1999 *Phys. Rev.* B **59** R11649
[53] Tohyama T and Maekawa S 2001 *Phys. Rev.* B **64** 212505
[54] Yokoyama H, Ogata M, Tanaka Y, Kobayashi K and Tsuchiura H 2013 *J. Phys. Soc. Jpn.* **82** 014707
[55] Chao K A, Spałek J and Oleś A M 1977 *J. Phys.* C **10** L271
[56] Feiner L F, Jefferson J H and Raimondi R 1996 *Phys. Rev.* B **53** 8751
[57] Foussats A and Greco A 2004 *Phys. Rev.* B **70** 205123
[58] Hubbard J 1963 *Proc. R. Soc. London* A **276** 238
[59] Morse D and Lubensky T 1991 *Phys. Rev.* B **43** 10436
[60] Merino J, Greco A, McKenzie R H and Calandra M 2003 *Phys. Rev.* B **68** 245121
[61] Bejas M, Greco A and Foussats A 2006 *Phys. Rev.* B **73** 245104
[62] Hybertsen M S, Stechel E B, Schluter M and Jennison D R 1990 *Phys. Rev.* B **41** 11068
[63] Affleck I and Marston J B 1988 *Phys. Rev.* B **37** 3774
[64] Affleck I and Marston J B 1989 *Phys. Rev.* B **39** 11538
[65] Yamase H and Kohno H 2000 *J. Phys. Soc. Jpn.* **69** 332
[66] Yamase H and Kohno H 2000 *J. Phys. Soc. Jpn.* **69** 2151
[67] Halboth C J and Metzner W 2000 *Phys. Rev. Lett.* **85** 5162
[68] Poilblanc D 2005 *Phys. Rev.* B **72** 060508
[69] Weber C, Poilblanc D, Capponi S, Mila F and Jaudet C 2006 *Phys. Rev.* B **74** 104506

[70] Macridin A, Jarrell M and Maier T 2006 *Phys. Rev.* B **74** 085104
[71] Koch E and Zeyher R 2004 *Phys. Rev.* B **70** 094510
[72] Hinton J P, Koralek J D, Yu G, Motoyama E M, Lu Y M, Vishwanath A, Greven M and Orenstein J 2013 *Phys. Rev. Lett.* **110** 217002
[73] Hinkov V, Haug D, Fauqué B, Bourges P, Sidis Y, Ivanov A, Bernhard C, Lin C T and Keimer B 2008 *Science* **319** 597
[74] Daou R, Chang J *et al* 2010 *Nature* **463** 519
[75] Onose Y, Taguchi Y, Ishizaka K and Tokura Y 2001 *Phys. Rev. Lett.* **87** 217001